ISSN 1063-780X, Plasma Physics Reports, 2008, Vol. 34, No. 3, pp. 199–202. © Pleiades Publishing, Ltd., 2008.
Original Russian Text © A.A. Letunov, V.P. Logvinenko, V.V. Zav'yalov, 2008, published in Fizika Plazmy, 2008, Vol. 34, No. 3, pp. 226–230.

PLASMA DIAGNOSTICS

Two-Color Terahertz Interferometer Based on the Frequency-Splitted Orthogonal Polarization Modes of the Water Vapor Laser and Designed for Measuring the Electron Density Profile in the L-2M Stellarator

A. A. Letunov[a], V. P. Logvinenko[a], and V. V. Zav'yalov[b]

[a] *Prokhorov Institute of General Physics, Russian Academy of Sciences, ul. Vavilova 38, Moscow, 119991 Russia*

[b] *P.L. Kapitza Institute for Physical Problems, Russian Academy of Sciences, ul. Kosygina 2, Moscow, 119334 Russia*

Received July 9, 2007

Abstract—An upgraded diagnostics for measuring the electron density profile in the L-2M stellarator is proposed. The existing diagnostics employs an interferometer based on an HCN laser with a mechanical frequency shifter and unmagnetized InSb detectors cooled with liquid helium. It is proposed to replace the HCN laser with a water vapor laser operating simultaneously at two wavelengths (220 and 118 μm). Being equipped with an anisotropic exit mirror, the water vapor laser allows the generation of orthogonally polarized, frequency-splitted modes at each of these wavelengths with a frequency difference of several tens of kilohertzs. Such a scheme makes it possible to get rid of the mechanical frequency shifter. Moreover, simultaneous measurements at two wavelengths allow one to reliably separate the phase increments introduced by the plasma electron component and by variations in the lengths of the interferometer arms. To take full advantage of this scheme, specially developed cryogenic receivers consisting of Ge and InSb photodetectors placed one after another will be used. To increase the response of the system near $\lambda = 220$ μm, the InSb detector is placed in a ≈0.55-T magnetic field.

PACS numbers: 52.70.Gw

DOI: 10.1134/S1063780X08030057

1. INTRODUCTION

The main parameters of the L-2M stellarator operating in the regime of electron cyclotron resonance heating (ECRH) are as follows [1]: the major radius is 1 m, the chamber minor radius is 17.5 cm, the average minor radius of the plasma column is 11.5 cm, the number of magnetic field periods is 14, the axial magnetic field is 1.34 T, the ohmic heating current is up to 20 kA, the gyrotron heating power is 100–300 kW, the gyrotron frequency is 75 GHz, and the axial electron density is $(0.5–3) \times 10^{13}$ cm^{-3}.

At present, the radial electron density profile in L-2M is measured with a multichord interferometer based on a 337-μm HCN laser [2–4]. The Michelson interferometer uses seven spherical mirrors installed inside the vacuum chamber. Scanning over chords is performed by rotating external mirror *8* (Fig. 1), which sequentially includes each mirror in the interferometer optical scheme. A disadvantage of this diagnostics is that it does not provide shine-trough probing over all the chords during one shot, because the stellarator winding does not allow one to make necessary diagnostic windows, thereby imposing serious limitations on the transportation of laser radiation through the chamber. The power of the HCN laser is ~10 mW. The phase shift is translated into the low-frequency range with the help of a mechanical Doppler shifter, which varies the laser frequency by 15 kHz. The radiation is recorded by unmagnetized InSb detectors cooled with liquid helium. The detector signals are digitized and are then processed by a PC. The system detectability (which corresponds to the minimum detectable phase increment caused by plasma electrons) is 5×10^{13} cm^{-2}.

Our purpose here was to improve the interferometer parameters, specifically, to improve the reconstruction of nonmonotonic radial density profiles and increase the accuracy of measurements at low plasma densities (including measurements along peripheral chords). An analysis shows that the measurement accuracy can be improved considerably by eliminating errors caused by uncontrollable changes in the lengths of the interferometer arms. This can be achieved by measuring the phase increment simultaneously at two wavelengths and by using probing radiation at shifted frequencies produced in the same laser cavity instead of made with an external mechanical frequency shifter.

All this can be done with the use of a special water vapor laser capable of generating frequency-splitted, orthogonally polarized modes at two wavelengths simultaneously [5].

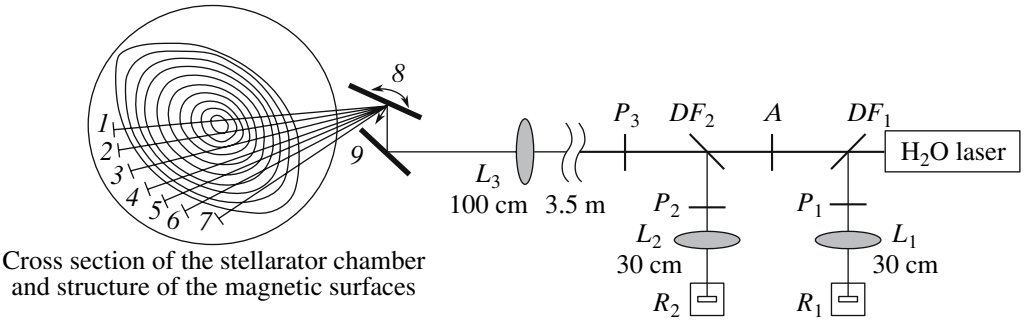

Fig. 1. Diagnostic system with an interferometer based on an H_2O laser: (*1*–*9*) mirrors, (L_1–L_3) polyethylene lenses, (P_1–P_3) polarizers, (DF_1, DF_2) dividing films, (*A*) attenuator, and (R_1, R_2) cryogenic receivers.

2. DIAGNOSTIC WATER VAPOR LASER AND APPROPRIATE RADIATION RECEIVERS

In [6], it was found that a continuous-wave water vapor laser could generate orthogonally polarized modes. This property was used to create a simple and reliable heterodyne interferometer [7, 8], which was successfully applied to measure the electron density profile in a microwave discharge in hydrogen and deuterium at pressures of a few atmospheres [8–10]. Lasing in the terahertz frequency range in water vapor discharges occurs on transitions between rotational levels in the vibrational bands of water molecules.

The exit grid mirror of the laser is made anisotropic with respect to the linear polarization of laser radiation. This is done by slightly stretching a square mesh along one of its diagonals without changing the lengths of the mesh sides (Fig. 2). In this case, the effective laser cavity length is different for different polarizations of an electromagnetic wave. As a result, each eigenmode of the cavity splits into two mutually orthogonal, linearly polarized components, whose orientation is determined by the anisotropy of the exit mirror.

This could be observed with a polarizer placed in the laser beam and oriented at an angle of 45° to the anisotropy direction. In this case, the photodetector signal revealed frequency beats between orthogonally polarized laser modes. The beat frequency was determined by the reflection-phase anisotropy and was in the range 3–300 kHz. Since both modes were excited in the same laser cavity, their frequency difference was very stable ($\delta\nu < 100$ Hz) and the axes of their spatial distributions coincided (Fig. 3).

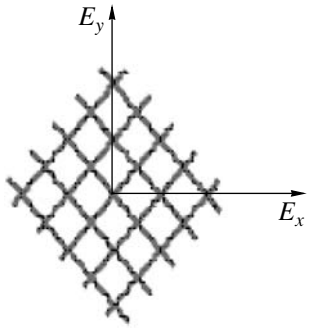

Fig. 2. Stretching of the meshes of the laser exit mirror along one of its diagonals without changing the length of the mesh side.

The divergence of the laser beam and the transverse distribution of its intensity are determined by the laser cavity modes. For the fundamental TEM_{00} mode we used, the intensity distribution is axisymmetric with a Gaussian radial profile of width $r(l)$, where l is the distance from the mirror plane. The power fraction within a circle of radius r is equal to $1 - \exp[-(r/r(l))^2]$. The beam width $r(l)$ is described by the expressions

$$r(l) = r_0\left(1 + \frac{l^2}{LR - L^2}\right)^{1/2},$$

$$r_0 = \left[\frac{\lambda}{4\pi}(LR - L^2)^{1/2}\right]^{1/2},$$

where r_0 is the beam radius at the plane mirror, L is the distance between the plane and spherical mirrors, R is the radius of curvature of the spherical mirror, and λ is the radiation wavelength.

Of practical interest is the effective radius of the beam holding 99% of its power, $r_{99} = 2.146r(l)$ (see Fig. 3). For our laser ($R = 7$ m, $L = 3.5$ m) and for wavelengths of 118.6 and 220 μm, the radius r_{99} on the plane mirror is equal to 12.3 and 16.8 mm, respectively.

The output mirror of our laser was a copper grid with a period of 40 μm, which produced beat frequencies of 38 and 81 kHz at the wavelength 200 and 118.6 μm, respectively. At these lines, output powers of 2 and 3 mW were obtained. By varying the pressure and composition of the gas mixture and adjusting the length of the laser cavity, one can achieve generation at one wavelength or simultaneously at several wavelengths by using the same exit mirror.

The beat frequencies at different wavelengths differ markedly, so the corresponding detector signals can be, in principle, discriminated by subsequent processing.

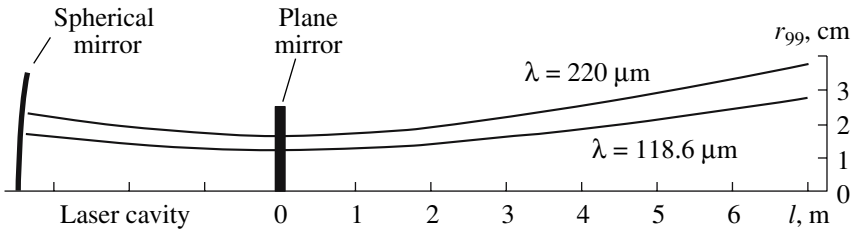

Fig. 3. Radius of the beam cross section holding 99% of the power of the operating laser lines.

However, to achieve the best sensitivity for each wavelength, it is more convenient to use different detectors. To detect radiation at the wavelengths 118.6 and 220 μm, we manufactured Ge and InSb photodetectors cooled with liquid helium [11]. Since the photoconductivity of Ge monocrystals has a long-wavelength cutoff at 120 μm, the Ge photodetector, being highly sensitive for the shorter wavelength laser radiation, is almost insensitive to the longer wavelength one.

In contrast, hot-electron InSb photodetectors are highly sensitive to the longer wavelength laser radiation. Moreover, their sensitivity can be increased considerably by placing the crystal in a magnetic field [12]. For this reason, we developed a sandwich-type receiver consisting of two crystals, Ge and InSb. Laser radiation is transmitted through a polished metal light guide with an inner diameter of 3.8 mm into a helium vessel. The receiver is mounted on the cooled end of the light guide. The InSb detector is placed in the field of a permanent magnet. At a magnetic field of $B = 0.55$ T, which is optimum for measurements, both the response to the 220-μm radiation and the InSb response ratio to the 220- and 118.6-μm lines are maximum. The beam radiation first passes through the Ge crystal, which is almost transparent to the 220-μm radiation. In this case, the selectivity of the detector increases because a lesser portion of the 118.6-μm radiation reaches the InSb crystal. The whole device is fabricated as an 11-mm-diameter insert for a commercial 10-liter Dewar vessel. At the upper end of the insert, there is a metal casing with four 50-Ω output preamplifiers powered from rechargeable batteries.

3. EXPERIMENTAL SETUP

Figure 1 shows a schematic of the experimental setup with the H_2O laser. The rear mirror of the laser cavity is a specular spherical mirror with the curvature radius $R = 7$ m. The exit mirror is made of a 40-μm copper mesh.

The interferometer is built according to the Michelson scheme with a set of return mirrors (or corner reflectors) installed inside the vacuum chamber.

The mesh, serving as a laser exit mirror, is oriented so that one of the mesh diagonals is vertical, whereas the other is horizontal. The reference signal is formed by a small portion of the laser power that is deflected by 20-μm Mylar dividing film DF_1 toward the receiver R_1 through 45° polarizer P_1. As polarizers, we used quasi-one-dimensional nickel grids with an operating period of 30 μm and transverse fasteners spaced by 340 μm. At both operating wavelengths, the grid transmits the radiation component polarized perpendicular to the long sides of the grid cells, whereas the other component is totally reflected.

Then, the laser beam enters the operating channel, where it is split by polarizer P_3. The horizontally polarized component passes into the stellarator, whereas the vertically polarized component is reflected back from the polarizer. The transmitted component passes twice through the plasma, being reflected from one of reflectors *1–7*, located inside the chamber, and then returns back through polarizer P_3. Divider DF_2 directs both these waves into a receiver R_2 through mixing polarizer P_2. The stellarator plasma gives rise to an additional phase shift in the operating channel. Attenuator *A*, installed between the dividers, reduces the fraction of radiation multiply passed through the plasma. This is very important because the laser exit mirror efficiently reflects radiation into the interferometer. The required beam radius in the transmission line is produced and maintained by polyethylene lenses L_1–L_3, whose transmittance is sufficient to align the system with the help of a visible-light laser.

During a stellarator discharge, the optical path of the probing beam varies due to the displacement of mirrors *1–7* under the action of the magnetic field pulse, thereby causing a parasitic phase shift. Simultaneous measurements at two wavelengths allow one to separate out the contribution made by the plasma electron component. This is the main destination of the two-wave interferometer.

4. CONCLUSIONS

The closest analogs of our two-wave interferometer are those designed at the Kurchatov Institute [13, 14] and NIFS [15]. In [15], two methanol (CH_3OD) lasers pumped by a CO_2 laser and operating at wavelengths of 57.2 and 47.6 μm are used. The use of these wavelengths is related, in particular, to the choice of the pumping line of the CO_2 laser and the necessity of its

precise maintenance. The frequency difference between pairs of laser lines (about 1 MHz) is maintained with an accuracy of 5 kHz by an active stabilization system, due to which the difference between the cavity lengths of these lasers varies by less than 1 nm. The interferometer is intended for use in ITER or in the upgraded LHD stellarator. A similar scheme was proposed in 1991 for use in the T-15 tokamak [13]. That version consisted of four lasers pumped by a CO_2 laser: two 185.6-μm CH_3OH lasers with a frequency difference of 600 kHz and two 119-μm CH_2F_2 lasers with a frequency difference of 900 kHz. In both schemes, all the beams were brought together by rather complicated optical systems.

Our version of a two-frequency interferometer, which is intended for the use in the L-2M stellarator, possesses similar capabilities but is simpler and more reliable in operation, because it uses only one laser.

Moreover, the use of a water vapor laser offers additional advantages: it can operate at different wavelengths, and the wide range of controllable displacements of the rear mirror (25 mm) without worsening the accuracy and stability of the angular adjustment allows simultaneous generation not only at two but also at three different wavelengths. The $H_2O + H_2$ laser provides continuous-wave generation at the following wavelengths [5–7]: 28.0, 33.0, 47.2, 55.1, 78.4, 79.1, 115, 118.6, and 220 μm, while the $D_2O + D_2$ laser can operate at the wavelengths 71.9, 84.3, 107.7, and 171.7 μm. Conditions for the generation of these lines, as well as their intensities, depend on the period and transmittance of the exit grid mirror. The 28-, 33-, and 84.3-μm lines correspond to transitions with $\Delta J = 1$; therefore, the modes with different linear polarizations are strongly coupled and their competition prevents simultaneous generation of orthogonally polarized modes with different frequencies. The generation of the other lines (which correspond to transitions with $\Delta J = 0$) by a laser of the given design was observed in [5–7]. Although the parameters of the grid mirrors were not optimized, the frequency difference at the 78.4-μm line reached 300 kHz.

At present, we have an operating laser and an appropriate radiation receiver at our disposal. Based on these components, we have assembled a test bench, at which we will test the performance of the interferometer. The plasma column will be simulated by a movable dielectric object, and the signals will be recorded with the L-2M data acquisition system. These tests will allow us to more correctly estimate the detectability of the interferometer. It is expected that the detectability will be improved two- to threefold (to $\sim 2 \times 10^{13}$ cm^{-2}). The next step will be the replacement of the existing L-2M interferometer with the newly developed one.

ACKNOWLEDGMENTS

This work was supported by the RF Presidential Program for Support of Leading Scientific Schools, grant no. NSh-5382.2006.2.

REFERENCES

1. S. E. Grebenshchikov, Tr. IOFAN **31**, 37 (1991).
2. A. D. Smirnova, Tr. IOFAN **31**, 175 (1991).
3. S. V. Kladov and A. D. Smirnova, Tr. FIAN **160**, 25 (1985).
4. A. V. Knyazev, A. A. Letunov, and V. P. Logvinenko, Prib. Tekh. Éksp., No. 2, 105 (2004) [Instrum. Exp. Tech. **47**, 230 (2004)].
5. V. V. Zav'yalov and G. D. Bogomolov, Prib. Tekh. Éksp., No. 3, 174 (1982).
6. V. V. Zav'yalov and G. D. Bogomolov, Pis'ma Zh. Éksp. Teor. Fiz. **20**, 393 (1974) [JETP Lett. **20**, 176 (1974)].
7. V. V. Zav'yalov, Cand. Sci. (Phys.–Math.) Dissertation (Kapitza Inst. for Physical Problems, USSR Acad. Sci., Moscow, 1976).
8. E. A. Tishchenko, V. V. Zav'yalov, V. G. Zatsepin, and V. B. Lasarev, in *Proceedings of the 13th International Conference on Phenomena in Ionized Gases, Berlin, 1977*, p. 161.
9. P. L. Kapitsa, Zh. Éksp. Teor. Fiz. **57**, 1801 (1969) [Sov. Phys. JETP **30**, 973 (1970)].
10. G. D. Bogomolov, Yu. V. Dubrovskiĭ, A. A. Letunov, and V. V. Peskov, Zh. Éksp. Teor. Fiz. **93**, 519 (1987) [Sov. Phys. JETP **66**, 295 (1987)].
11. V. V. Zav'yalov, E. A. Zotova, and E. Yu. Shamparov, Prib. Tekh. Éksp., No. 2 (2008) (in press).
12. G. D. Bogomolov, V. V. Zav'yalov, E. A. Zotova, and E. Yu. Shamparov, Prib. Tekh. Éksp., No. 1, 87 (2002) [Instrum. Exp. Tech. **45**, 78 (2002)].
13. Z. Vereshchinski, V. G. Gerasimov, E. P. Gorbunov, et al., Fiz. Plazmy **18**, 198 (1992) [Sov. J. Plasma Phys. **18**, 106 (1992)].
14. E. P. Gorbunov and Yu. V. Skosyrev, in *Proceedings of the 5th International Symposium on Laser-Aided Plasma Diagnostics, Bad-Honnef, 1991*, p. 139.
15. K. Kawahata, K. Tanaka, T. Tokuzawa, et al., Rev. Sci. Instrum. **75**, 3508 (2004).

Translated by N.F. Larionova